DNA-Network-Templated Self-Assembly of Silver Nanoparticles and Their Application in Surface-Enhanced Raman Scattering

Gang Wei, Li Wang, Zhiguo Liu, Yonghai Song, Lanlan Sun, Tao Yang, and Zhuang Li*

State Key Laboratory of Electroanalytical Chemistry, Changchun Institute of Applied Chemistry, Graduate School of the Chinese Academy of Sciences, Chinese Academy of Sciences, Changchun 130022 China

Received: August 23, 2005; In Final Form: October 8, 2005

A large-scale λ-DNA network on a mica surface was successfully fabricated with a simple method. Silver nanoparticles capped with the cationic surfactant cetyltrimethylammonium bromide (CTAB) were self-assembled onto a two-dimensional DNA network template by electrostatic interaction and formed nanoporous silver films, which can be used as active surface-enhanced raman scattering (SERS) substrates. Two probe molecules, Rhodamine 6G (R6G) and 4-aminothiophenol (4-ATP), were studied on these substrates with very low concentrations, and great enhancement factors for R6G ($0.21 \times 10^{10}-4.09 \times 10^{11}$) and 4-ATP ($\sim 1.70 \times 10^{5}$) were observed. It was found that the enhancement ability was affected by the DNA concentration and the electrostatic absorption time of the CTAB-stabilized silver nanoparticles on the DNA strands. These SERS substrates formed by the self-assembly of silver nanoparticles on DNA network also show good stability and reproducibility in our experiments.

1. Introduction

Surface-enhanced Raman scattering (SERS) has been shown to be a useful tool for the detection of low-concentration analytes, sometimes even achieving single-molecule sensitivity.[1−5] To date, the main challenge is how to prepare SERS-active substrates that can provide great detection sensitivity and be stable, reproducible, inexpensive, and easy to prepare.[4,6] Different SERS-active substrates have been prepared and applied for the detection of chemical and biological molecules.[7−23] Usually, in addition to providing controllable nanoscale roughness to allow for the excitation of the surface plasmon, a solid SERS active substrate must offer a vast surface area and open porous structure. On the basis of these two crucial factors, several efficient and reliable SERS substrates have been fabricated using a nanoporous material coated with gold or silver layer.[24−26] For example, Tessier et al. fabricated thin porous gold films on glass substrates using a colloidal crystal template.[24] Chan et al. and Lin et al. produced SERS-active substrates based on immersion plating of silver onto porous silicon wafers.[25,26] These substrates all showed great Raman enhancement and could be used to detect chemical and biological molecules at very low concentrations.

A DNA network, as shown in previous works,[27,28] has nanoporous structures similar to those of the nanoporous silver or gold films prepared by Tessier et al.,[24] Chan et al.,[25] and Lin et al.[26] On the other hand, it was reported that DNA can be used as an excellent building block for the construction of one- and two-dimensional inorganic or semiconducting nanostructures.[29−35] In the work reported here, nanoporous silver films were prepared by the electrostatic self-assembly of silver nanoparticles capped with cetyltrimethylammonium bromide (CTAB) onto a DNA network template. It was found that these silver films could be used as good SERS-active substrates with Rhodamine 6G (R6G) and 4-aminothiophenol (4-ATP) as test probes, and the Raman enhancement ability can increase with the action time of the silver nanoparticles on the DNA network.

* To whom correspondence should be addressed. Fax: +86 431 5262057. Tel.: +86 431 5262057. E-mail: zli@ciac.jl.cn.

2. Experimental Section

Materials. Silver nitrate (AR), sodium borohydride (AR), ethanol (GR), methanol (GR), and cetyltrimethylammonium bromide (AR) were purchased from Beijing Chemical Co. (Beijing, China). Rhodamine 6G (R6G) was purchased from Exciton Chemical Co. Inc. (Dayton, OH). 4-Aminothiophenol (4-ATP) was obtained from Aldrich. λ-DNA (48502 bp, 400 ng/μL) was supplied by Sino-American Biotechnology Company (Beijing, China). All of these chemicals and materials were used as received. The water used throughout this work was ultrapure water (18 MΩ^{-1}) produced by a Milli-Q system.

Preparation of 30 ng/μL and 100 ng/μL λ-DNA Networks on Mica. λ-DNA networks were prepared with a simple method. Briefly, λ-DNA was diluted to 30 and 100 ng/μL with ultrapure water, and 15 μL of this DNA solution was dropped onto freshly cleaved mica. Five minutes later, the sample was rinsed with 3 mL of ethanol and ultrapure water for 30 s each. In this work, the 100 ng/μL DNA network has a more uniform nanoporous structure than the 30 ng/μL DNA network.

Several Nanoporous Silver Films Prepared by Electrostatic Self-Assembly of CTAB-Capped Silver Nanoparticles. CTAB-capped silver nanoparticles were prepared by a one-step reaction in an ethanol/water system. In brief, 2 mL of CTAB ethanol solution (1 mM) was mixed with 30 mL of silver nitrate (5 mM) under vigorous stirring. After 10 min, freshly prepared aqueous sodium borohydride solution (1%) was added to the mixed solution until the color of the colloids changed to yellow-green and the color did not change when more sodium borohydride was added.

Three silver films were prepared by templating with a 100 ng/μL DNA network by changing the adsorption time of the CTAB-capped silver nanoparticles on the DNA strands. First, 3 mL of freshly prepared bulk silver nanoparticles was added

10.1021/jp054752x CCC: $30.25
Published on Web 11/24/2005

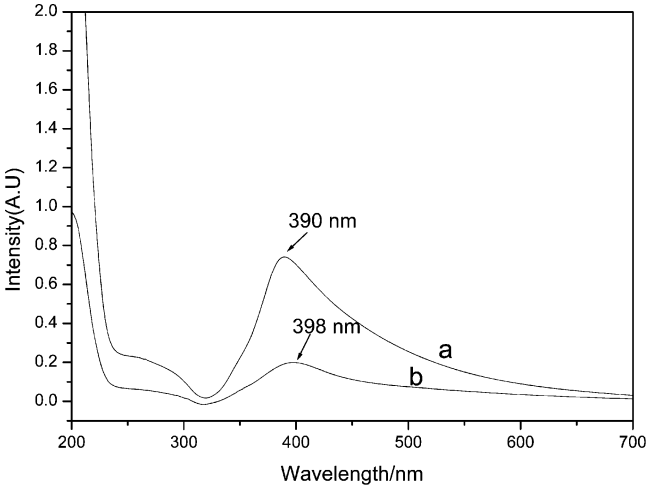

Figure 1. UV−vis spectra of silver nanoparticles (a) before and (b) after being capped with CTAB.

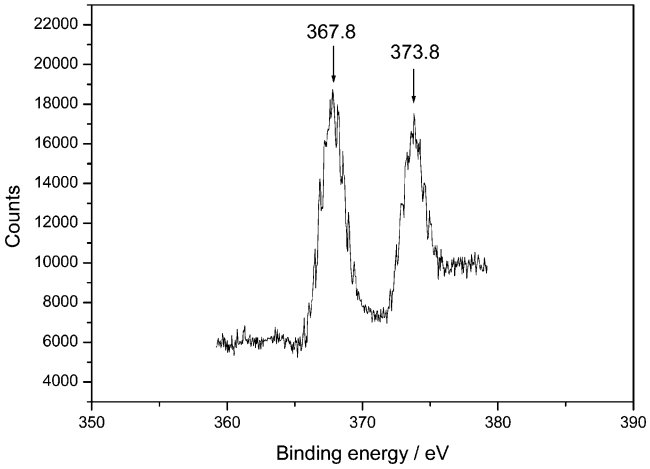

Figure 2. XPS spectrum of Ag 3d of the prepared CTAB-capped silver nanoparticles deposited on a mica substrate.

to a 5-mL test tube, and mica covered with DNA network was immersed into the silver colloid for different amounts of time, namely, 1 h for the 30 ng/μL DNA network and 30 min, 1 h, and 2 h for the 100 ng/μL DNA network. Then, the samples were rinsed with ethanol twice and dried under nitrogen gas. AFM was used to characterize the surface structure of these self-assembled silver films.

SERS Measurements of R6G and 4-ATP on These Silver Films. R6G solution was diluted to various concentrations ranging from 1×10^{-9} to 1×10^{-14} M with methanol, and then 20 μL of each solution was dropped onto a nanoporous silver film, and the solvent was allowed to evaporate under ambient conditions. 4-ATP solution was diluted to different concentrations ranging from 1×10^{-5} to 1×10^{-7} M with ethanol. Again, 20 μL of each solution was dropped onto a nanoporous silver film, and the solvent was allowed to evaporate under ambient conditions. These treatments were done for the different nanoporous silver films formed by changing the electrostatic absorption time. Finally, a Raman spectrometer was used to measure the SERS activities of these silver films directly. In this experiment, more than five SERS-active substrates of each silver film were prepared, and 10 different points on each substrate were selected to detect the R6G and 4-ATP probes, to verify the stability and reproducibility of these SERS active substrates.

Instruments. UV−visible absorbance spectra were collected using a UV-2450 spectrophotometer (Shimadzu Corporation, Kyoto, Japan). X-ray photoelectron spectroscopy (XPS) was conducted on a VG ESCALAB MK II spectrometer (VG Scientific, Crawley, U.K.) employing monochromatic Mg Kα radiation as the X-ray source ($h\nu = 1253.6$ eV). Tapping-mode AFM imaging was performed on a Digital Instruments multimode AFM controlled by a Nanoscope IIIa apparatus (Digital Instruments, Santa Barbara, CA) equipped with an E scanner. A standard silicon cantilever tip from Digital Instruments was used. The scan rate was 1−1.5 Hz. SERS spectra were measured with a Renishaw 2000 model confocal microscopy Raman spectrometer with a CCD detector and a holographic notch filter (Renishaw Ltd., Gloucestershire, U.K.). Radiation of 514.5 nm from an air-cooled argon ion laser was used for the SERS excitation.

3. Results and Discussion

3.1. Synthesis and Characterization of CTAB-Capped Silver Nanoparticles. Figure 1a shows the UV−vis spectrum of silver nanoparticles synthesized without capping reagents. The silver colloid exhibits a well-defined surface plasmon band with a maximum absorbance at ~390 nm, which is similar to that previously reported for silver nanoparticles formed by the reduction of sodium citrate.[36] Unfortunately, however, the nanoparticles synthesized by this method could not exist stably, and precipitation would occur after about 30 min. The synthesized CTAB-capped silver nanoparticles exhibited a strong plasmon resonance peak at 398 nm, as shown in Figure 1b. The red shift is due to the formation of a conjugated structure between the silver nanoparticles and the CTAB molecules.

Figure 2 presents the XPS spectrum of CTAB-capped silver nanoparticles deposited on mica. The Ag 3d spectrum consists of two components with binding energies (BEs) of 367.8 and 373.8 eV, which agrees very well with the Ag $3d_{5/2}$ core-level binding energy.[37−39] The low-BE component is assigned to metallic Ag, and the higher-BE component can be assigned to CTAB-capped Ag, which is expected to form a concentric shell of CTAB around the Ag core. The XPS data strongly agreed with the UV−vis data and supported the formation of CTAB-capped silver nanoparticles.

Atomic force microscopy (AFM) was used to measure the size of the CTAB-capped silver nanoparticles. Figure 3a shows the AFM image of CTAB-capped silver nanoparticles deposited onto mica. A section analysis indicates the size of particles is about 22 nm. Figure 3b shows the statistical histogram of the size of the silver particles, which is about 20.58 ± 2.68 nm. It should be noted that the dimensions of the particles were measured according to the height but not width because the AFM tip radius will affect the measurement.

3.2. Preparation of λ-DNA Networks and Electrostatic Self-Assembly of CTAB-Capped Silver Nanoparticles Templated with λ-DNA Networks. The preparation of the λ-DNA networks was simple. DNA was dropped onto freshly cleaved mica, and 5 min later, it was treated with ethanol for about 1 min. The posttreatment with ethanol is very important for two basic reasons. One reason is that ethanol can thoroughly dehydratethe DNA network; then, the binding force of the DNA strands on the negatively charged mica is so strong that the DNA network is retained even after being soaked in water. Another reason is that ethanol can remove the DNA absorbed onto other DNA but does not remove the DNA absorbed on the mica surface.[27] Figure 4a,b shows typical AFM images of DNA networks with different DNA concentrations. When the DNA concentration is 30 ng/μL, the DNA strands crossed over

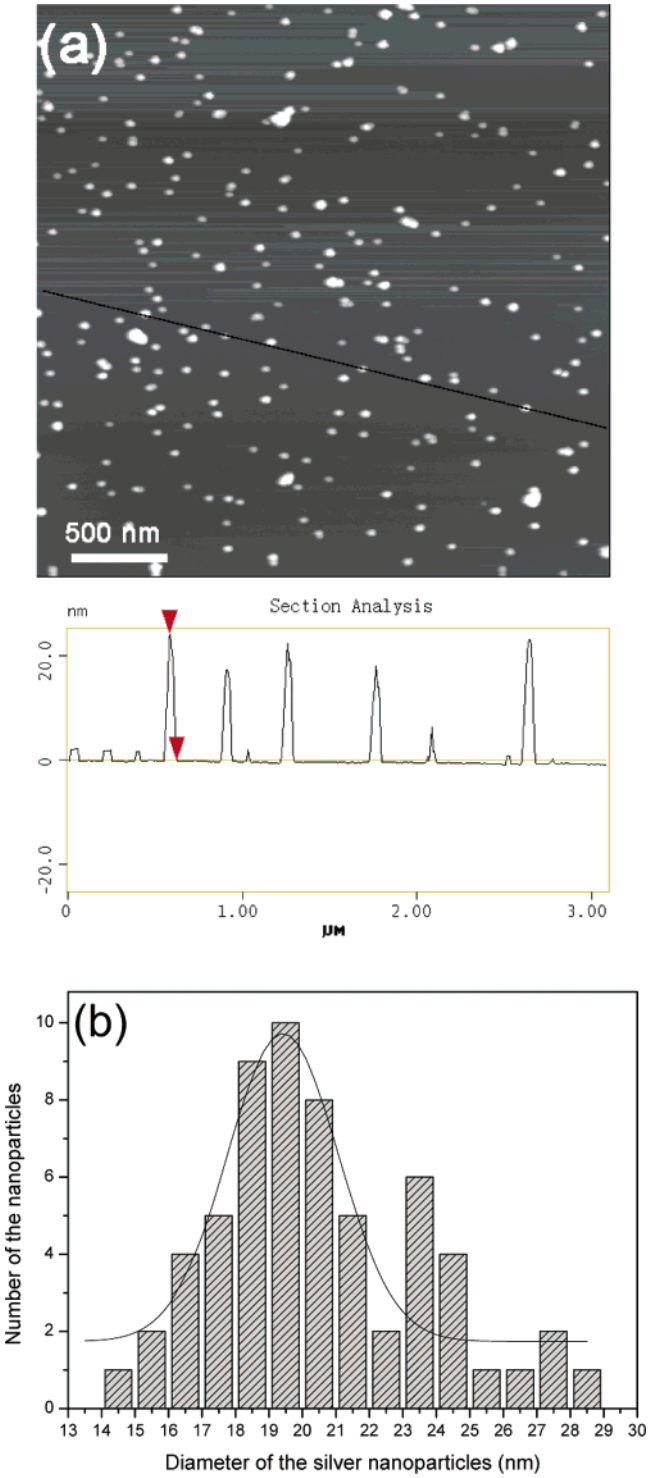

Figure 3. (a) Typical AFM image and (b) histogram of CTAB-capped silver nanoparticles deposited on freshly cleaved mica. A section analysis reveals the diameter of the particles to be about 22 nm.

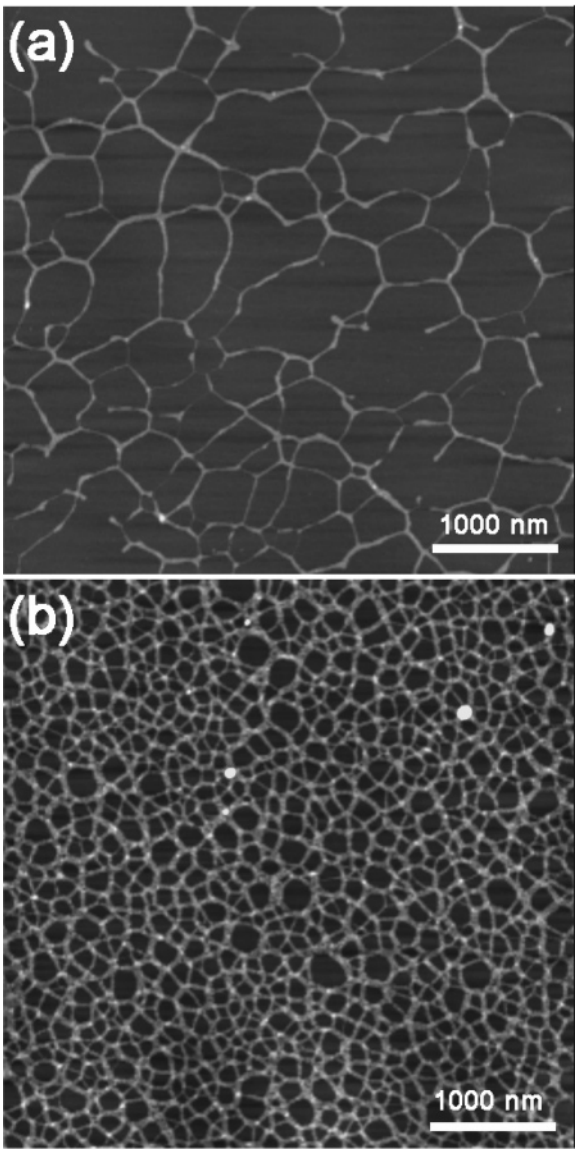

Figure 4. Typical AFM images of λ-DNA networks with different DNA concentrations: (a) 30 and (b) 100 ng/μL. The z-scale bar is 10 nm for both images.

together simply and formed a netlike structure. When the DNA concentration was increased to 100 ng/μL, a DNA network with a uniform strand height and mesh was obtained. A section analysis indicated that the strand height was about 1.6 and 2.3 nm for Figure 4a and b, respectively. As reported in previous articles, the height of double-stranded DNA spread on mica is about 0.4−0.7 nm measured by AFM in tapping mode.[40,41] We concluded that the height data reflect 2−4 and 3−5 DNA strands overlapping each other for the 30 and 100 ng/μL DNA networks, respectively. On the other hand, for the 30 ng/μL DNA network, the mesh size changes from 157 nm to 1.48 μm, as shown in Figure 4a. In contrast, for the 100 ng/μL DNA network, the mesh was generated with a uniform size and strand height, and a statistical analysis indicated that the mesh size was about 154 ± 50 nm. Compared to the DNA network in Figure 4a, an important change in Figure 4b is the increase in the DNA strand height and the decrease in the diameter of the mesh in the DNA network. The 100 ng/μL network provides a better template for the formation of compact and uniform nanoporous silver films by the electrostatic assembly of silver nanoparticles on DNA strands.

CTAB-capped silver nanoparticles were self-assembled onto the DNA strands by electrostatic interactions of the negatively charged phosphate DNA backbone and positively charged silver nanoparticles. Figure 5a,b shows typical AFM images of self-assembled silver films obtained by absorbing CTAB-capped silver particles onto the 30 and 100 ng/μL DNA networks, respectively. The two images clearly confirm that CTAB-stabilized silver nanoparticles were absorbed onto the DNA strands with high specificity. It was also found that, with increasing DNA concentration, such as from 30 to 100 ng/μL,

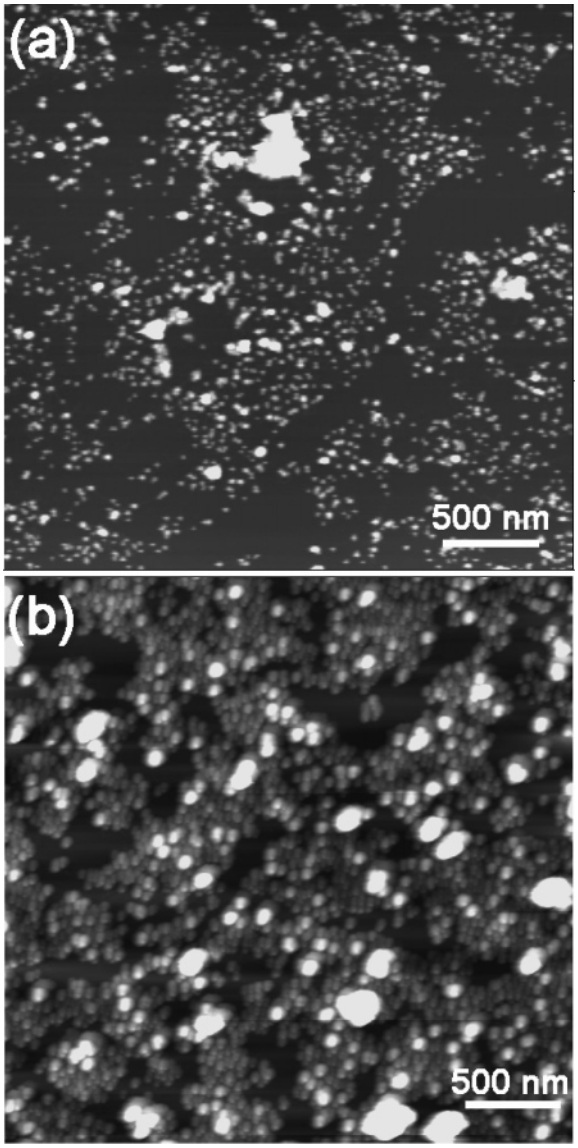

Figure 5. Tapping-mode AFM images of self-assembled silver films obtained by absorbing CTAB-capped silver particles onto a DNA network: (a) 30 and (b) 100 ng/μL for 1 h. The *z*-scale bar is 40 nm in both images.

the assembled silver nanoparticles became denser on the DNA strands and the silver films were formed from a microporous structure to a nanoporous structure.

In the space where no DNA was present, nearly no silver nanoparticles adsorbed, as shown in Figure 5a. It is obvious that the interactions between the DNA and the nanoparticles are predominant over those between the mica and the nanoparticles. By using this specific character of DNA and CTAB-capped silver particles, we have fabricated silver-nanoparticle-coated DNA nanowires.[42] In our experiments, however, the DNA chains are nearly invisible, which might be due to the increase in background roughness caused by the adsorption of silver nanoparticles. Without question, many factors will affect the electrostatic assembly of silver nanoparticles on DNA strands, such as colloid concentration, incubation time, solution pH, and capping reagent selection, among others. In this work, the main purpose was to provide a simple and efficient approach for the preparation of SERS substrates; optimal conditions for the self-assembly of nanoparticles will be investigated in the future.

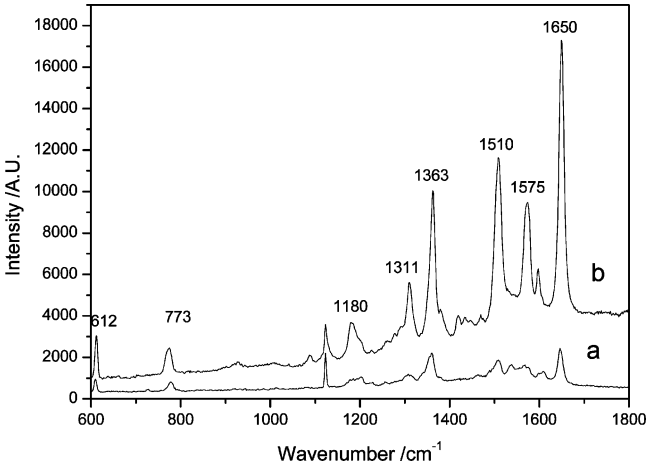

Figure 6. Typical SERRS spectra of (a) 1×10^{-11} M R6G on the silver films formed on the 30 ng/μL DNA network and (b) 1×10^{-12} M R6G on the nanoporous silver film on the 100 ng/μL DNA network. Laser power, 25 mW, 1%; integration time, 30 s.

3.3. SERS Measurements of R6G and 4-ATP on These Nanoporous Silver Films. The nanoporous silver films can be readily used as substrates for surface-enhanced Raman scattering (SERS) for molecular sensing with high sensitivity and specificity. Two target molecules, R6G and 4-ATP, were used to investigate the SERS sensitivity of these substrates. It should be noted that the Raman signal of R6G molecules partly contributes to the resonance enhancement (about 2−3 orders of magnitude) of the laser used, such as the 514.5-nm argon ion laser used in our work, so the spectrum of R6G detected is actually the surface-enhanced resonance Raman scattering (SERRS) signal. Figure 6a shows the SERRS spectrum of 1×10^{-11} M R6G on macroporous silver film (the AFM image was shown in Figure 5a), and Figure 6b shows the SERRS spectrum of 1×10^{-12} M R6G on nanoporous silver film (the AFM image was shown in Figure 5b). In these two SERS-active substrates, low-concentration R6G produced a clear enhanced effect at 1650 cm^{-1}, one of the main characteristic bands. A detailed assignment of the spectral features of R6G has been reported previously and will not be repeated here.[43]

The effect of different times of absorption of CTAB-capped silver nanoparticles on the DNA networks was considered. Figure 7a−c show the larger-scale optical microscope images of silver films formed by assembling silver nanoparticles on DNA networks (100 ng/μL) for 30 min, 1 h, and 2 h, respectively. It is obvious that more compact silver films were formed with increasing incubation time between the DNA network and the CTAB-capped silver nanoparticles. Figure 8a−c presents the SERRS spectra of 1×10^{-12} M R6G collected from the substrates shown in Figure 7a−c, respectively. An obvious trend is that the enhancement ability increases with increasing incubation time, with the intensity of the band at 1650 cm^{-1} in Figure 8b and c being enhanced 2-fold and 4-fold, respectively, compared to that in Figure 8a.

A control experiment was also performed to confirm the importance of the nanoporous silver films in the enhancement ability. Newly cleaved mica was incubated with silver colloid for 1 h, and R6G was used to detect the enhancement activity of this substrate. No SERS signal was observed when the concentration of R6G was 1×10^{-12} M. Even when the R6G concentration was increased to 1×10^{-9} M under the same conditions, an interpretable Raman signal was still not obtained (data not shown). Therefore, we suggest the great Raman enhancement of R6G on this nanoporous film is attributed to

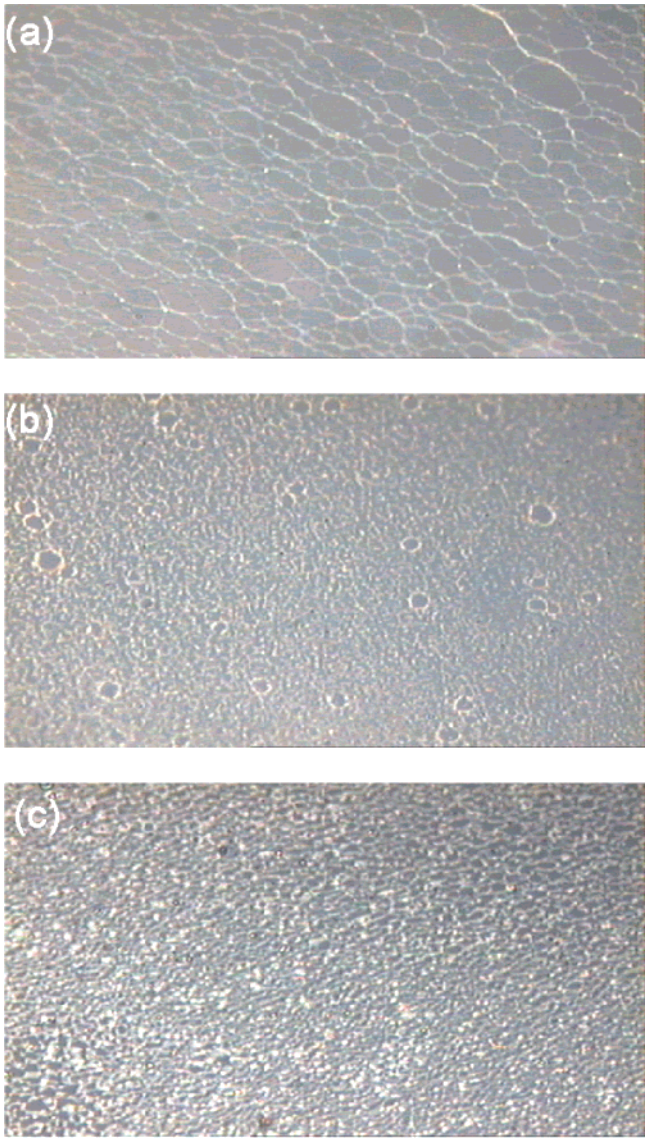

Figure 7. Typical optical microscope images (500×) of silver films formed by the self-assembly of CTAB-stabilized silver nanoparticles on a 100 ng/μL DNA network for (a) 30 min, (b) 1 h, and (c) 2 h. The image scale is 100 μm × 56 μm.

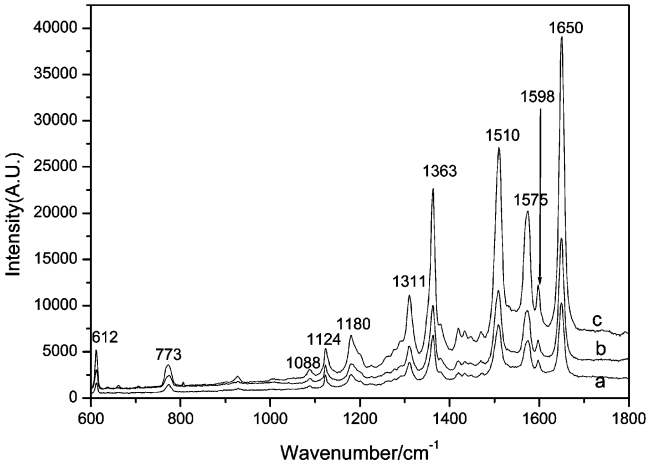

Figure 8. SERRS spectra of R6G (1×10^{-12} M) on silver films formed by the self-assembly of CTAB-stabilized silver nanoparticles on a 100 ng/μL DNA network for (a) 30 min, (b) 1 h, and (c) 2 h, as indicated in Figure 7. Laser power, 25 mW, 1%; integration time, 30 s.

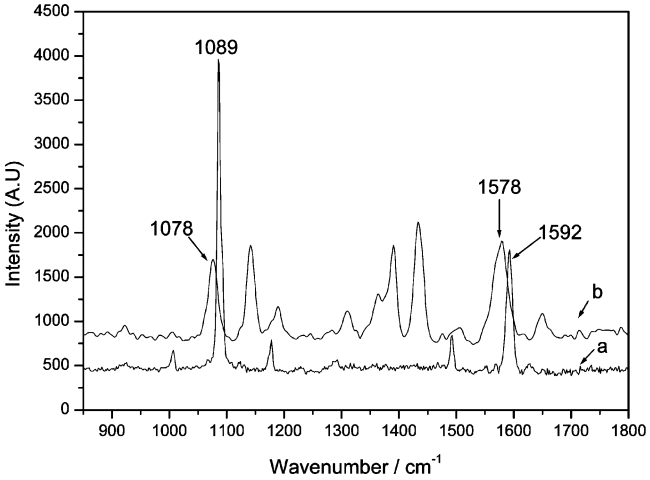

Figure 9. Comparison of normal Raman spectrum and SERS spectrum of 4-ATP. (a) Normal Raman spectrum of solid sample. (b) SERS spectrum of 4-ATP (1×10^{-7} M) on the active substrate prepared as Figure 7b. Laser power, 25 mW, 1%; integration time: 30 s.

two main causes. One is the formation of nanoscale pores on the silver film. It has been reported that great SERS enhancements were obtained on silver-coated silicon nanopores and nanostructured gold film templated by colloidal crystals.[24−26] Compared to the SERS-active gold and silver films, nanoporous silver films will provide a broader surface plasmon resonance for optical scattering and cause the enhancement of electromagnetic field, as reported by Musick et al.[44] Another cause is the formation of some silver nanoparticle aggregations on the DNA network, as shown in Figure 5b. Indeed, the electric enhancement might occur between two or more aggregated colloids.[44] The enhancement mechanism is similar to that reported in the studies of Brus et al., who performed the surface-enhanced Raman spectroscopy of individual R6G molecules on large silver nanocrystals aggregates of 10−15 nanoparticles.[7−9] In our work, DNA cannot directly cause the aggregation of CTAB-capped silver nanoparticles. When DNA is immobilized on the surface of mica, it is difficult for the DNA conformation to change, which does not provide a suitable situation for the aggregation of silver nanoparticles. In fact, as shown in Figure 7, the particles were likely assembled on the DNA strands in the early stage and then became aggregated with the particles in the colloid.

Figure 9 displays the normal Raman spectrum of solid 4-ATP and the SERS spectrum of 4-ATP on the nanoporous silver film prepared by incubating a DNA network with silver colloid for 1 h. The normal Raman spectrum (Figure 9a) of solid 4-ATP is similar to that reported by Osawa et al. and Zheng et al.[45,46] Relative to the spectrum obtained in the solid, the noticeable differences in the SERS spectrum (Figure 9b) on the nanoporous silver film are the frequency shifts for some changes in band intensity. The ν_{CS} band shifts from 1089 cm^{-1} in Figure 9a to 1077 cm^{-1} in Figure 9b, and an obvious Raman frequency shift from 1592 to 1578 cm^{-1} was also observed. These changes of several main bands indicate that the −SH group in 4-ATP makes direct contact with the silver film surface by forming a strong Ag−S bond. It should be noted that the SERS-active substrates can greatly enhance the Raman signals of R6G and 4-ATP, but there is no SERS signal from the templating DNA or from the CTAB. We think this might be a result of the experimental conditions in our work, such as the concentration of DNA or CTAB used, the wavelength and power of the laser, the integration time, and so on.

TABLE 1: SERS Enhancement Factors (EFs) of the Silver Films Formed in This Experiment for R6G and 4-ATP

substrate (DNA network on mica)	R6G (at 1650 cm^{-1})	4-ATP (at 1078 cm^{-1})
30 ng/μL, 1 h absorption	0.21×10^{10}	
100 ng/μL, 30 min absorption	1.07×10^{11}	
100 ng/μL, 1 h absorption	1.70×10^{11}	1.70×10^{5}
100 ng/μL, 2 h absorption	4.09×10^{11}	

The enhancement factors (EFs) for 4-ATP and R6G on the substrate prepared by 1 h of incubation were calculated according to the following equation[47,48]

$$\mathrm{EF} = \frac{I_{\mathrm{SERS}}}{I_{\mathrm{Raman}}} \frac{M_{\mathrm{bulk}}}{M_{\mathrm{surface}}}$$

where I_{SERS} and I_{Raman} are the intensities in the SERS and normal Raman spectrum, respectively; M_{bulk} is the concentration of molecules in the bulk sample; and M_{surface} is the concentration of adsorbed molecules. For the target molecule 4-ATP, in the sample area (1 μm in diameter) measured, M_{surface} was calculated to be $1.2 \times 10^4/\mu m^2$. Taking the laser spot (1 μm in diameter) and the penetration depth (about 2 μm) and the density of 4-ATP (1.17 g/mL) into account,[49] M_{bulk} had a value of $0.82 \times 10^{10}/\mu m^3$ in the detected solid sample area. For the vibrational mode at 1089 cm^{-1} (ν_{CS}), an EF of 1.70×10^5 was obtained. In this work, the ratio of the Raman intensities of the R6G- and thiol-related C−C stretching bands at R6G saturation coverage was about 1×10^6, as reported by Tao et al.[47] Using this ratio and the EF for 4-ATP, the EF for R6G was estimated to be 1.70×10^{11} for the silver film formed by 1 h of absorption of CTAB-stabilized silver nanoparticles. Measuring from the Raman spectra shown in Figures 6, 8, and 9, the probable SERS enhancement factors (EFs) for these silver films formed in our experiment were determined, as shown in Table 1. In fact, many factors will affect the Raman enhancement, such as the size, aggregation, and assembly pattern of the particles. Therefore, it is important to control the aggregation of the particles and the pattern of the assembly in order to obtain more reproducible Raman signals.

The use of our DNA-network-mediated silver films as SERS substrates has several advantages. First, the preparation of the DNA network is simple, and the substrate is formed by the direct self-assembly of the nanoparticles onto the DNA network. Second, the features of the silver film are strongly based on those of the DNA network, and it is possible to achieve larger field enhancement factors by adjusting the height and mesh size of the DNA network. Last, the silver films reveal stronger SERS activities and higher signal-to-noise ratios and can detect single molecules of R6G. In our recent study, we synthesized silver nanoparticles, nanorods, and nanowires on DNA networks by the direct reduction of silver nitrate. The silver nanoparticles formed on the DNA network template on modified mica could be used as SERS substrates, and a typical probe molecule, R6G (1×10^{-8} M), showed a clear enhanced effect at 1650 cm^{-1}.[50] Hence, the DNA-network-mediated preparation of SERS substrates described in this work could have potential applications in chemical and biological analysis, as well as medical detection.

4. Conclusions

In summary, we have fabricated microporous and nanoporous silver films simply by the electrostatic self-assembly of CTAB-capped silver nanoparticles onto a λ-DNA network. It was revealed that the nanoporous silver films could be used as stable and reproducible SERS-active substrates. SERS measurements of small-molecule probes, such as R6G and 4-ATP, were performed on these substrates with high sensitivity and reproducibility. The great Raman enhancements achieved on these new substrates are believed to be the result of the formation of nanoporous structures on the silver film and the aggregation of the silver nanoparticles.

Acknowledgment. This work was supported by the National Natural Science Foundation of China.

References and Notes

(1) Graham, D.; Smith, W. E.; Linacre, A. M. T.; Munro, C. H.; Watson, N. D.; White, P. C. *Anal. Chem.* **1997**, *69*, 4703.
(2) Emory, S. R.; Nie, S. *Science* **1997**, *275*, 1102.
(3) Kneipp, K.; Wang, Y.; Kneipp, H.; Perelman, L. T.; Itzkan, I.; Dasari, R. R. Feld, M. S. *Phys. Rev. Lett.* **1997**, *78*, 1667.
(4) Kneipp, K.; Kneipp, H.; Itzkan, I.; Dasari, R. R.; Feld, M. S. *Chem. Rev.* **1999**, *99*, 2957.
(5) Vo-Dinh, T.; Allain, L. R.; Stokes, D. L. *J. Raman Spectrosc.* **2002**, *33*, 511.
(6) Campion, A.; Kambhampati, P. *Chem. Soc. Rev.* **1998**, 241.
(7) Michaels, A. M.; Nirmal, M.; Brus, L. E. A. *J. Am. Chem. Soc.* **1999**, *121*, 9932.
(8) Michaels, A. M.; Jiang, J.; Brus, L. *J. Phys. Chem. B* **2000**, *104*, 1196.
(9) Jiang, J.; Bosnick, K.; Maillard, M.; Brus, L. *J. Phys. Chem. B* **2003**, *107*, 9964.
(10) Leopold, N.; Lendl, B. *J. Phys. Chem. B* **2003**, *107*, 5723.
(11) Kneipp, K.; Kneipp, H.; Manoharan, R.; Hanlon, E. B.; Itzkan, I.; Dasari, R. R.; Feld, M. S. *Appl. Spectrosc.* **1998**, *52*, 1493.
(12) Faulds, K.; Littleford, R. E.; Graham, D.; Dent, G.; Smith, W. E. *Anal. Chem.* **2004**, *76*, 592.
(13) Albrecht, M. G.; Creighton, J. A. *J. Am. Chem. Soc.* **1977**, *99*, 5215.
(14) Jeanmaire, D. L.; Duyne, R. P. V. *J. Electroanal. Chem.* **1977**, *84*, 1.
(15) Leung, L. H.; Weaver, M. J. *J. Am. Chem. Soc.* **1987**, *109*, 5113.
(16) Grochala, W.; Kudelski, A.; Bukowska, J. *J. Raman Spectrosc.* **1998**, *29*, 681.
(17) Sanchez-Cortes, S.; Garcia-Ramos, J. V. *Langmuir* **2000**, *16*, 764.
(18) Saito, Y.; Wang, J. J.; Smith, D. A.; Batchelder, D. N. *Langmuir* **2002**, *18*, 2959.
(19) Schlegel, V. L.; Cotton, T. M. *Anal. Chem.* **1991**, *63*, 241.
(20) Roy, D.; Barber, Z. H.; Clyne, T. W. *J. Appl. Phys.* **2002**, *91*, 6085.
(21) Leverette, C. L.; Shubert, V. A.; Wade, T. L.; Varazo, K.; Dluhy, R. A. *J. Phys. Chem. B* **2002**, *106*, 8747.
(22) Li, X. L.; Zhang, J. H.; Xu, W. Q.; Jia, H. Y.; Wang, X.; Yang, B.; Zhao, B.; Li, B. F.; Ozaki, Y. *Langmuir* **2003**, *19*, 4285.
(23) Li, X. L.; Xu, W. Q.; Zhang, J. H.; Jia, H. Y.; Yang, B.; Zhao, B.; Li, B. F.; Ozaki, Y. *Langmuir* **2004**, *20*, 1298.
(24) Tessier, P. M.; Velev, O. D.; Kalambur, A. T.; Rabolt, J. F.; Lenhoff, A. M.; Kaler, E. W. *J. Am. Chem. Soc.* **2000**, *122*, 9554.
(25) Chan, S.; Kwon, S.; Koo, T. W.; Lee, L. P.; Berlin, A. A. *Adv. Mater.* **2003**, *15*, 1595.
(26) Lin, H. H.; Mock, J.; Smith, D.; Gao, T.; Sailor, M. J. *J. Phys. Chem. B* **2004**, *108*, 11654.
(27) Kanno, T.; Tanaka, H.; Miyoshi, N.; Kawai, T. *Appl. Phys. Lett.* **2000**, *77*, 3848. Nakayama, Y.; Tanaka, H.; Kawai, T. *Jpn. J. Appl. Phys.* **2001**, *40*, 824.
(28) Wu, A. G.; Li, Z.; Yu, L. H.; Wang, H. D.; Wang, E. K. *Anal. Sci.* **2001**, *17*, 583. Wu, A. G.; Li, Z.; Zhou, H. L.; Zheng, J. P.; Wang, E. K. *Analyst* **2002**, *127*, 585. Wu, A. G.; Li, Z.; Wang, E. K. *Anal. Sci.* **2004**, *20*, 1083. Wu, A. G.; Cheng, W. L.; Li, Z.; Jiang, J. G.; Wang, E. K. *Talanta* **2005**, in press.
(29) Braun, E.; Eichen, Y.; Sivan, U.; Ben-Yoseph, G. *Nature* **1998**, *391*, 775.
(30) Ford, W. E.; Harnack, O.; Yasuda, A.; Wessels, J. M. *Adv. Mater.* **2001**, *13*, 1793.
(31) Willner, I.; Patolsky, F.; Wasserman, J. *Angew. Chem., Int. Ed.* **2001**, *40*, 1861.
(32) Mirkin, C. A.; Letsinger, R. L.; Mucic, R. C.; Storhoff, J. J. *Nature* **1996**, *382*, 607.
(33) Niemeyer, C. M. *Science* **2002**, *297*, 62.
(34) Le. J. D.; Pinto, Y.; Seeman, N. C.; Musier-Forsyth, K.; Taton, T. A. Kiehl, R. A. *Nano Lett.* **2004**, *4*, 2343.
(35) Maeda, Y.; Tabata, H.; Kawai, T. *Appl. Phys. Lett.* **2001**, *79*, 1181.
(36) Lee, P. C.; Meisel, D. *J. Phys. Chem.* **1982**, *86*, 3391.
(37) Gole, A.; Sainkar, S. R.; Sastry, M. *Chem. Mater.* **2000**, *12*, 1234.
(38) Kumar, A.; Pattarkine, M.; Bhadbhade, M.; Mandale, A. B.; Ganesh, K. N.; Datar, S. S.; Dharmadhikari, C. V.; Sastry, M. *Adv. Mater.* **2001**, *13*, 341.

(39) Kumar, A.; Mandale, A. B.; Sastry, M. *Langmuir* **2000**, *16*, 6921.
(40) Thundat, T.; Allison, D. P.; Warmack, R. J. *Nucleic Acids Res.* **1994**, *22*, 4224.
(41) Hansma, H. G.; Revenko, I.; Kim, K.; Laney, D. E. *Nucleic Acids Res.* **1996**, *24*, 713.
(42) Wei, G.; Wang, L.; Zhou, H.; Liu, Z.; Song, Y.; Li, Z. *Appl. Surf. Sci.* **2005**, in press.
(43) Hildebrandt, P.; Stockburger, M. *J. Phys. Chem.* **1984**, *88*, 5935.
(44) Musick, M. D.; Keating, C. D.; Lyon, L. A.; Botsko, S. L.; Pena, D. J.; Holliway, W. D.; McEvoy, T. M.; Richardson, J. N.; Natan, M. J. *Chem. Mater.* **2000**, *12*, 2869.
(45) Osawa, M.; Matsuda, N.; Yoshll, K.; Uchida, I. *J. Phys. Chem.* **1994**, *98*, 12702.
(46) Zheng, J.; Li, X.; Gu, R.; Lu, T. *J. Phys. Chem. B* **2002**, *106*, 1019.
(47) Tao, A.; Kim, F.; Hess, C.; Goldberger, J.; He, R.; Sun, Y.; Xia, Y.; Yang, P. *Nano Lett.* **2003**, *3*, 1229.
(48) He, P.; Liu, H.; Li, Z.; Liu, Y.; Xu, X.; Li, J. *Langmuir* **2004**, *20*, 10260.
(49) Yu, H. Z.; Zhang, J.; Zhang, H. L.; Liu, Z. F. *Langmuir* **1999**, *15*, 16.
(50) Wei, G.; Zhou, H.; Liu, Z.; Song, Y.; Wang, L.; Sun, L.; Li, Z. *J. Phys. Chem. B* **2005**, *109*, 8738.